

## **IoT-Based Safety Monitoring and Display System for Aluminium Electrolysis Cell Bypass Shunts**

**Qing Wei<sup>1</sup>, Shanyong Chen<sup>2</sup>, Junbiao Shi<sup>3</sup>, Jinguo Wang<sup>4</sup>, Hao Wang<sup>5</sup> and Chen Chen<sup>6</sup>**

1. Senior Engineer

Zhengzhou Non-ferrous Metals Research Institute of Chalco (ZRI), Zhengzhou, China

3. Professor, vice director

4., 5. Senior Engineers

Chinalco (Baotou) Aluminium, Baotou, China

6. Engineer

Chinalco (Zhengzhou) Aluminium, Zhengzhou, China

Corresponding author: Chen Chen, 2297544304@qq.com

<https://doi.org/10.71659/icsoba2025-al022>

### **Abstract**

The cell bypass shunts of an aluminium electrolytic cell are used for shutting down a cell when it needs relining. In normal operation the bypass shunts are insulated from anode risers so that the cell current can flow from the cathode busbars to the anode beam of the downstream cell. When the voltage across the bypass shunt becomes excessive or when the insulation performance deteriorates, it may trigger electrical arcs, leading to, in severe cases, melting of the bypass shunt and potline open circuit. Therefore, real-time monitoring of the bypass shunt condition is an indispensable aspect of the electrolytic production process. However, in actual production, the inspection of bypass shunts primarily relies on manual efforts, which not only involves high labor intensity but also poses significant safety risks.

To address this issue, the Zhengzhou Nonferrous Metals Research Institute of Chinalco has successfully developed an intelligent monitoring and display system for aluminium electrolytic cell bypass shunts, based on Internet of Things (IoT) technology. This system consists of three components: a wireless network transmission unit, a bypass shunt detection unit, and a visual display unit. The bypass shunt detection unit utilizes partial discharge detection technology and acoustic fingerprint recognition to continuously and real-time monitor the insulation status and discharge conditions of each bypass shunt. The detected data is transmitted to the visual display system via the wireless network unit. The wireless network unit employs a multi-hop MESH network based on Zigbee communication technology, effectively addressing the complex and harsh communication conditions in aluminium electrolytic production environments. The visual display unit supports visualization on various digital terminals, including PCs and mobile devices. In the event of anomalies, it promptly issues warning messages to assist in rapid fault diagnosis, thereby effectively preventing bypass shunt explosions.

The application of this system enables digital and intelligent real-time monitoring of the bypass shunt status in aluminium electrolytic cells, improving greatly smelter operation safety and reliability.

**Keywords:** Aluminium electrolysis, Cell bypass shunts, Internet of Things (IoT), Safety monitoring.

### **1. Introduction**

As the core equipment in aluminium electrolysis production, the insulation status of aluminium reduction cell bypass shunts directly impacts both, production efficiency and operational safety. All Chinese cell technologies have the bypass shunts at the base of anode risers (Figure 1).

Figure 2 is schematic representation of bypass shunts in PC software interface. During normal operation, insulation failure at bypass shunts can cause partial current leakage to adjacent cells, resulting in energy loss. During cell preheat, poor contact at bypass shunts may lead to uneven current distribution, potentially causing potline current fluctuations that affect the entire potline efficiency. More critically, when a pot tap-out occurs or anodes are pulled out of the bath, an open circuit occurs and the potline voltage can appear at bypass shunts, potentially triggering explosive accidents with significant economic losses and safety hazards.

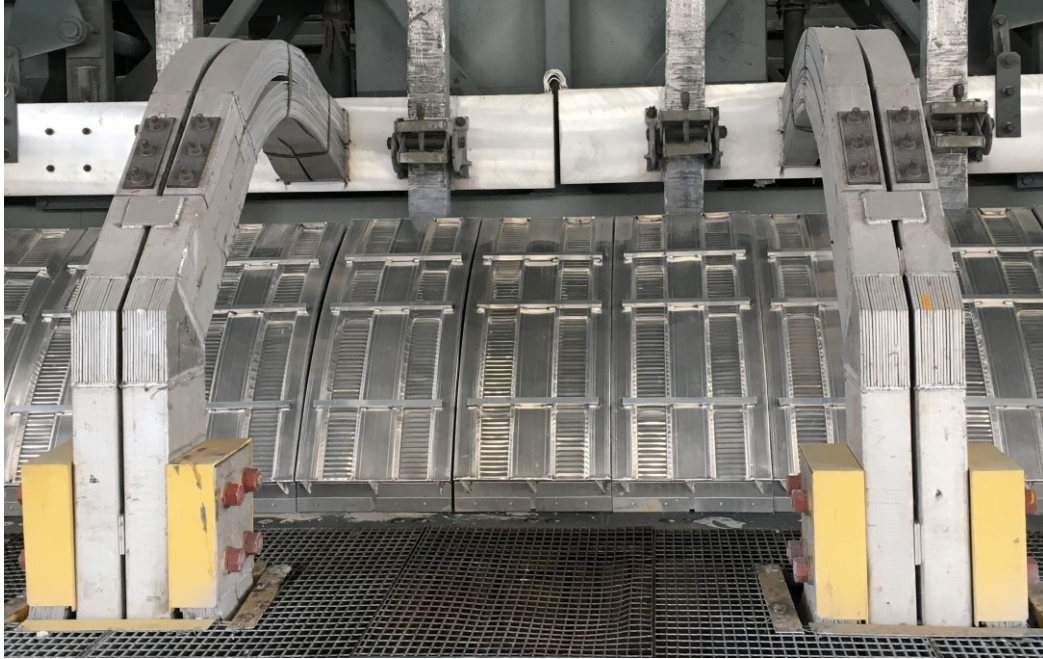


**Figure 1. Anode risers and bolted bypass shunts at the base of the risers in a Chinese cell technology. Shunt insulation is yellow.**

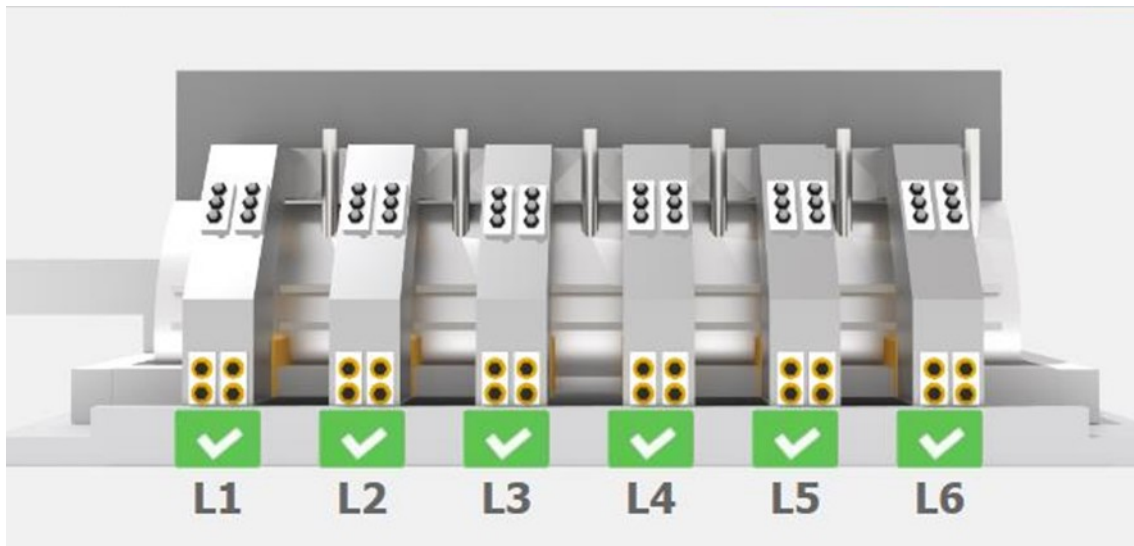


**Figure 2. Schematic representation of anode risers and bypass shunts at the base of the risers (shunt is yellow, bolts are black) for a cell with 6 risers, as displayed in PC software interface. Green squares with checkmarks show that the shunt have no problem.**

Figure 3 shows statistics of bypass shunt failures [1].

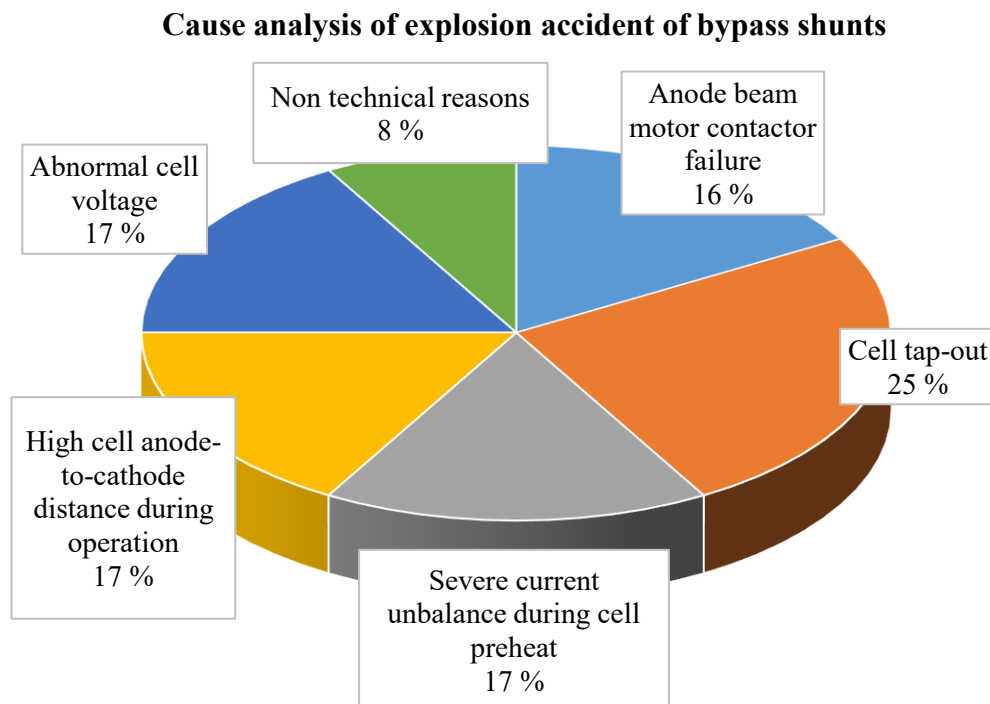


**Figure 3. Classification of explosion causes of the cell bypass shunts [1].**

Given these risks, aluminium smelters prioritize bypass shunts monitoring. However, traditional manual inspection methods face three major limitations:

- 1) Poor timeliness – relying on periodic shutdown inspections makes it impossible to detect sudden insulation degradation;
- 2) Insufficient accuracy – manual measurements lack sensitivity to weak discharges (< 50 pC) and early-stage acoustic signals (< 40 dB);
- 3) High risk – the high-temperature, strong electromagnetic environment in potrooms poses threats to inspection personnel.

To address these challenges, the Zhengzhou Nonferrous Metals Research Institute of CHINALCO has developed an advanced monitoring and protection system for cell bypass shunts. This innovative system utilizes information technology to prevent bypass shunt explosions, replacing manual inspections to eliminate potential hazards, ensure production safety, and prevent significant economic losses.

## **2. Analysis of Typical Bypass Shunt Fault Types and Monitoring Methods in Aluminium Reduction Cells**

Bypass shunts have different states at different stages of electrolytic production. When the electrolytic cell is producing, the bypass shunt should be in a high resistance state, and the current flows into the electrolytic cell from the anode risers and anodes and then flows out from the cathode after undergoing a reduction reaction with the electrolyte. When the electrolytic cell is under maintenance, the bypass shunt should be in a short-circuit state. At this time, the current no longer flows into the current electrolytic cell, but flows through the bypass shunt busbar to the next electrolytic cell.

## 2.1 Typical Faults at Bypass Shunts

### 2.1.1 Insulation Degradation Fault

**Dust accumulation:** Metal dust (such as Al, Fe particles), carbon dust, form conductive channels on the surface of the insulation board, leading to partial discharge (PD). Experimental data shows that when the dust thickness is greater than 0.5 mm, the initial discharge voltage decreases by 40 % (from 60 V to 36 V).

**Insulation aging:** Epoxy resin insulation boards undergo carbonization at high temperatures (> 150 °C), resulting in a decrease in resistivity from  $10^{13}$  to  $10^6 \Omega \cdot m$ .

### 2.1.2 Electrical Breakdown Fault

**Surface flashover:** When the creepage distance of the insulation bolt surface is insufficient, flashover occurs at the anode effect voltage (> 50 V), and typical cases show that the peak flashover current can reach 3 kA (duration 2 ms).

**Metal erosion:** Poor contact of the bypass shunt busbar leads to local overheating (> 300 °C), causing the aluminium busbar to melt and form an arc.

### 2.1.3 Mechanical Structural Faults

**Stress deformation:** Thermal cycling stress causes the bypass shunt insulation board to warp and deform by more than 2 mm, resulting in uneven insulation gaps (measured data: for every 1 mm increase in deformation, the probability of arc discharge increases by 25 %).

## 2.2 Analysis of Fault Detection Methods

At present, the main methods for detecting faults at bypass shunts include insulation resistance detection, local pulse detection, ultrasonic detection, and red hair imaging detection. The existing detection methods have their own characteristics but also have certain limitations. To evaluate the engineering applicability of different technologies, this section compares and analyses mainstream fault detection methods from three aspects: detection principles, sensitivity, and practical application bottlenecks (Table 1).

**Table 1. Analysis of insulation fault detection methods for cell bypass shunts.**

Method	Applicable Faults	Sensitivity	Limitations
Insulation resistance	Bulk insulation failure	>1 k $\Omega$ ( $\pm 10$ % error)	Cannot locate localized defects
Partial discharge (PD) [2]	Early-stage dust discharge	Detects $\geq 5$ pC	Susceptible to EMI (>30 dB noise)
Ultrasonic testing	Mechanical loosening/arcing	20–200 kHz range	Requires couplant; complex setup
Infrared thermography	Contact overheating	0.1°C resolution	Fails for non-thermal faults

From the above table, it can be seen that a single detection method is difficult to fully cover the complex fault modes of bypass shunts. For example, although insulation resistance measurement can reflect the overall insulation level, its sensitivity to early partial discharge (<10 pC) is insufficient. Although ultrasonic testing can capture mechanical loosening characteristics, it is difficult to achieve full coverage monitoring due to installation limitations.

### 3. System Design

In response to the above issues, this article proposes an intelligent monitoring system for bypass shunts based on the Internet of Things architecture. The development of the system was supported by references [2–8]. The system logic diagram is shown in Figure 4, which includes the perception layer, transport layer, platform layer, and application layer.

The perception layer deploys intelligent terminals such as insulation resistance monitoring devices, partial discharge sensors, and infrared temperature measurement devices to collect real-time multi-dimensional data from short intersections. The transmission layer uses industrial grade Zigbee wireless Mesh network and fibre ring network dual channel redundant transmission to ensure reliable data transmission in complex electromagnetic environments. Build a cloud-based data centre at the platform level, integrating data storage, AI analysis, and digital twin simulation functions. The application layer achieves real-time monitoring of status, graded alarms, and maintenance decision support through a PC/mobile visual interface, forming a closed-loop control system of "end edge cloud" collaboration.

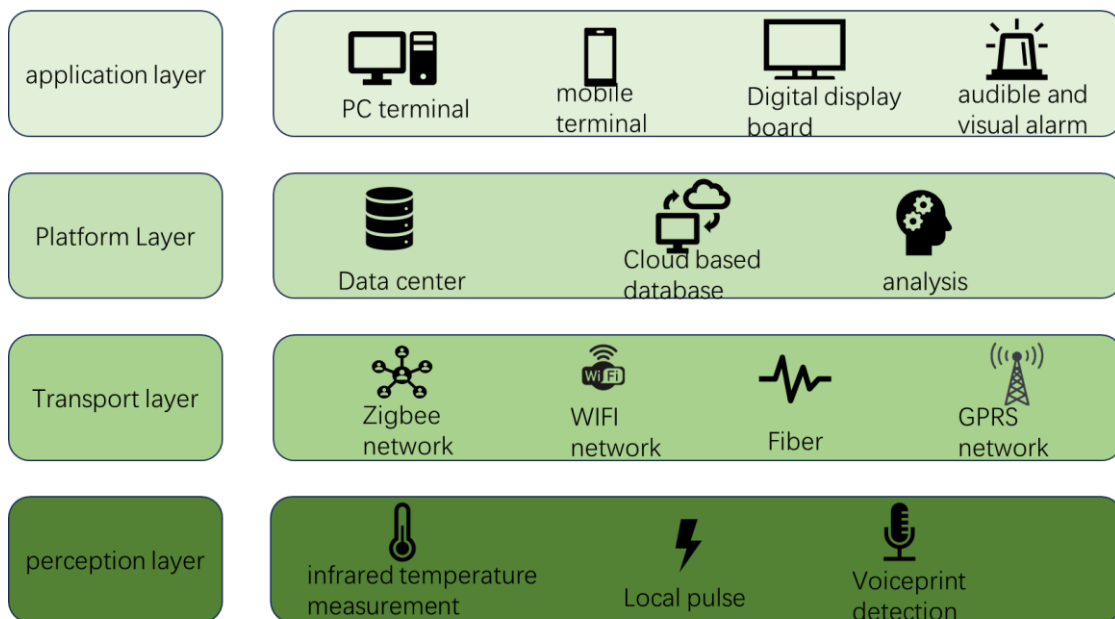


Figure 4. Logic block diagram of intelligent monitoring system for cell bypass shunts.

#### 3.1 Perception Layer Hardware Design

The hardware design of the aluminium electrolytic cell bypass shunt monitoring system uses a modular distributed architecture, with multi parameter sensing terminals deployed at each bypass shunt. The insulation monitoring unit consists of high-frequency current sensors (HFCT) and embedded insulation resistance detection modules, which are installed on both sides of the grounding wire and insulation board, respectively. The temperature monitoring uses a dual redundancy scheme of infrared thermal imager and fibre optic temperature probe, achieving

scanning of 0.5 m × 0.5 m area and contact temperature measurement of key points at 800 °C. Mechanical condition monitoring captures vibration and abnormal noise signals through three-axis MEMS accelerometers and explosion-proof microphone arrays. All sensor data is locally pre-processed by the industrial edge computing gateway (ARM Cortex-A72 core) and uploaded through Zigbee MESH network. The hardware system meets the IP67 protection level, ensuring stable operation in strong magnetic fields and highly corrosive environments in the potroom. Sensor options are shown in Table 2.

**Table 2. Selection table of sensors for intelligent monitoring system at bypass shunts.**

Monitoring Parameter	Sensor Type	Installation Location	Technical Specifications
Insulation resistance	Online megohmmeter	Both sides of bypass shunt insulation plate	Range: 0–1000 MΩ, accuracy: ±1 %
Partial discharge	High Frequency Current Transformer (HFCT)	Bypass shunt grounding line	Bandwidth: 1–50 MHz, sensitivity: 0.1 pC
Temperature	Infrared thermometer	Conductor connections, insulation surface	Measuring range: -20–600 °C, accuracy: ±1 °C
Vibration/Acoustic	MEMS Accelerometer + microphone array	Bypass shunt metal frame	Frequency range: 20 Hz–20 kHz
Ambient humidity	Explosion-proof humidity sensor	Near bypass shunt	Range: 0–100 %RH, accuracy: ±2 %

### 3.2 Transport Layer Network Architecture

The transport layer uses an industrial grade multi-mode heterogeneous network architecture, which forms a dual channel redundant transmission system through Zigbee wireless Mesh self-organizing network (compliant with IEEE 802.15.4g standard) and fiber ring network. Each edge computing node, as the relay station of the Mesh network, supports multi hop routing, achieves 200m radius coverage in the strong electromagnetic interference environment of the electrolytic workshop, and the packet loss rate is less than 0.1 %. Key data synchronization is carried out through a 4-core armoured optical cable (OS2 single-mode fibre) for backbone transmission, using a ring topology design, with a switching time of less than 50 ms when a single point of fibre breakage occurs. The network layer is equipped with adaptive frequency hopping algorithm (2.4 GHz frequency band, 16 channel polling) and time division multiple access (TDMA) protocol, ensuring end-to-end delay of less than 100 ms when more than 200 nodes are connected simultaneously, meeting the real-time alarm requirements for emergency events such as insulation breakdown. All communication interfaces are equipped with surge protectors and magnetic ring filters to ensure reliable operation in harsh environments of the electrolysis workshop.

### 3.3 Platform Layer Service Construction

The platform layer uses a cloud based collaborative microservice architecture, built on an industrial PaaS platform, and includes three core modules: real-time data lake, AI analysis engine, and digital twin. The data lake achieves the collection and storage of tens of thousands of data points per second through time-series databases and distributed file systems. The AI analysis engine integrates multiple model containers such as insulation life prediction (random forest algorithm) and fault diagnosis (LSTM neural network) and supports online incremental learning. The platform uses container orchestration to achieve elastic scheduling of computing resources, and interfaces with MES/ERP systems through standard interfaces to form a closed-loop

management of "monitoring warning decision-making operation and maintenance". The overall response delay is controlled within 50 0ms, meeting the real-time requirements of industry

### 3.4 Application Layer Software Design

The application layer uses a multi terminal collaborative interaction design, and achieves full scene monitoring through a web-based visualization platform and a mobile app. The web-based platform is based on integrated 3D digital twin views, real-time trend curves (with millisecond refresh support), and intelligent diagnostic report dashboards. The mobile end uses cross platform technology and has the functions of sound and light vibration multi-mode alarm push and emergency operation guidance. The system supports role-based interface configuration (three-level permissions of operator/engineer/administrator) and integrates with enterprise digital systems to achieve automatic dispatch of inspection work orders. At the same time, it provides API interfaces for DCS system to call, forming a full process closed-loop management of "monitoring alarm disposal feedback", with human-machine interaction response time controlled within 1 second.

## 4. Industrial Testing

This system underwent a 6-month industrial test in a large smelter 400 kA potline. Figures 5 and 6 show the installation of data collection and data transmission modules in the basement. The system was deployed in 6 test cells (Potroom A) and compared with 6 traditional monitoring cells (Potroom B). At the beginning of the experiment, baseline data collection was conducted for a period of 2 weeks, and key parameter benchmark values such as insulation resistance (450–600 M $\Omega$ ), contact surface temperature (85–110 °C), and vibration characteristics (main frequency 120–150 Hz) were obtained under normal operating conditions. To verify the sensitivity of the system, artificial fault simulations were conducted in weeks 3–4, including inducing insulation degradation by spraying NaF containing electrolytic dust solution (resistance value decreased from 520 M $\Omega$  to 65 M $\Omega$  for 53 hours), and simulating mechanical faults by loosening connecting bolts. The system was able to provide timely warnings, with the insulation resistance triggering a first level alarm when it decreased to 82 M $\Omega$ , and mechanical loosening faults identified within 2 hours after the appearance of 250 Hz abnormal harmonics in the vibration spectrum.

Figures 7 and 8 show real-time digital display and PC software interface.



**Figure 5. Cell bypass shunt data collection module.**



**Figure 6. Data transmission terminal.**



**Figure 7. Real-time digital display board.**



**Figure 8. PC software interface.**

In the subsequent natural working condition monitoring, the system successfully captured three real insulation breakdown events. In the most typical example, the partial discharge pulse suddenly increased from 5 pC to 210 pC. The system issued a warning 36 hours in advance, and the breakdown position located by the infrared thermal imager was less than 3 cm away from the actual position. Experimental data showed that the use of intelligent monitoring reduced the number of insulation fault shutdowns in Potroom A pots by 85.7 % (from 2.1 times/cell-month to 0.3 times/cell-month), reduced temperature exceeding events by 88.2 %, and saved 87.5 % of manual inspection time. In contrast, a cell bypass shunt accident occurred during the traditional manual inspection of Potroom B, resulting in a 6-hour shutdown of the potline.

The experiment shows that the fault warning of this system is accurate. During the experiment, three insulation breakdown accidents were successfully avoided with a warning 12–72 hours in advance (the alarm was triggered when the insulation resistance value decreased from 500 M $\Omega$  to 82 M $\Omega$ ), and the accuracy of mechanical loosening identification reached 96.7 % (the comparison result of vibration spectrum characteristics). The production efficiency has significantly improved, with an 83 % reduction in unplanned shutdowns related to bypass shunts during the trial period (only one unexpected power outage occurred during the trial period, compared to an average of five for traditional production lines during the same period). By avoiding bypass shunt losses, the DC energy consumption can be reduced by 27 kWh/t Al. The system also significantly reduces the workload of manual inspections, reducing the frequency of manual inspections from 2 times per shift to once per week. The fault location time has been shortened to less than 15 minutes (traditional methods require 4–8 hours). The system can run stably and reliably, with a fault-free operation time of more than 4000 hours in an environment with the potroom temperature of 65 °C and magnetic field of 10 mT (100 gauss). The wireless transmission packet loss rate is stably controlled to below 0.08 %.

## 5. Conclusions

The intelligent monitoring system for the bypass shunts of the aluminium reduction cell, designed and implemented in this research comprises real-time monitoring and fault early warning of the cell bypass shunts through multi-sensor fusion, edge computing and cloud collaborative analysis. This system can provide fault warning and safety assurance for aluminium electrolysis production, identify bypass shunt insulation degradation in advance, and achieve success rate of 96.7 % in diagnosing mechanical looseness. Energy efficiency is improved, and economic benefits are reduced metal production loss due to short-circuits, and 27 kWh/t Al reduction in DC power consumption. The intelligent operation and maintenance transformation has been achieved, and the manual inspection frequency of this system has been reduced by 85 %. The fault location time has been shortened from the hourly level to 15 minutes, confirming the feasibility of the "predictive maintenance" mode.

## 6. References

1. Wei Qing et al., System development and application for preventing the explosion of aluminium reduction cell bypass shunts, *Proceedings of the 39th International ICSOBA Conference*, 22–24 November 2021, *Travaux* 50, 889–896.
2. Sepp Hochreiter, Jürgen Schmidhuber, Long Short-Term Memory, *Neural Computation* 1997, 9 (8), 1735–1780. doi: <https://doi.org/10.1162/neco.1997.9.8.1735>.
3. Leo Breiman, Random Forests, *Machine Learning* 2001, 45, 5–32, <https://doi.org/10.1023/A:1010933404324>.
4. Pablo E. Aqueveque, Eduardo P. Wiechmann and Rolando P. Burgos, Short-Circuit Detection for Electrolytic Processes Employing Optibar Intercell Bars, *IEEE Transactions on Industry Applications*, Vol. 45, No. 4, 1225–1231, July–August 2009, <https://doi.org/10.1109/TIA.2009.2023357>.
5. Luiz A.M.M. Nobrega et al. Design and Development of a Bio-Inspired UHF Sensor for Partial Discharge Detection in Power Transformers, *Sensors* 2019,19 653, <https://doi.org/10.3390/s19030653>.
6. Helmy Fitriawan et al., ZigBee based wireless sensor networks and performance analysis in various environments, *2017 15th International Conference on Quality in Research (QIR), International Symposium on Electrical and Computer Engineering*, Nusa Dua, Bali, Indonesia, 2017, 272–275, <https://doi.org/10.1109/QIR.2017.8168495>.
7. Liling Hou. Design and implementation of a remote monitoring system for wireless sensor networks based on ZigBee [J]. *Journal of Changchun Institute of Technology* (Natural Science Edition), 2015, 16 (4), 32–35.
8. Lian, Wu and Lee Jong Han, Multimedia Application and Network Architecture Design Based on Multiterminal Collaboration, *Journal of Signal Processing Systems*, 2022, Vol. 94, 131–143, <https://doi.org/10.1155/2022/7997773>.

